Fabrication of a Cell Fixation Device for Robotic Cell Microinjection

Yu Xie *, Yunlei Zhou, Wenming Xi, Feng Zeng and Songyue Chen

School of Aerospace Engineering, Xiamen University, Xiamen 361005, China;
19920141152932@stu.xmu.edu.cn (Y.Z.); wmxi@xmu.edu.cn (W.X.);
19920141152946@stu.xmu.edu.cn (F.Z.); s.chen@xmu.edu.cn (S.C.)
* Correspondence: xieyu@xmu.edu.cn; Tel.: +86-151-6006-1679

Abstract: Automation of cell microinjection greatly reduces operational difficulty, but cell fixation remains a challenge. Here, we describe an innovative device that solves the fixation problem without single-cell operation. The microarray cylinder is designed with a polydimethylsiloxane (PDMS) material surface to control the contact force between cells and the material. Data show that when the injection velocity exceeds 1.5 mm/s, microinjection success rate is over 80%. The maximum value of the adhesion force between the PDMS plate and the cell is 0.0138 N, and the need can be met in practical use of the robotic microinjection.

Keywords: PDMS; microinjection; robotic; contact force

1. Introduction

Microinjection allows the administration of a foreign target gene directly into the nucleus of a fertilized egg using a glass needle under a microscope to integrate the foreign gene into the recipient cell genome. This is a common biological procedure, used in in vitro fertilization and transgenic technology [1]. Historically, the traditional technique involved transferring cells with a microsuction tube under a microscope and microinjecting with a needle smaller than 10 μm in diameter [2]. However, this required specific skills and time and effort. Recently, Sun and Dong's groups reported successful automation of this technique [3–6]. Specifically, a motor drives the needle to completely inject the cell, and the cell injection force or microscope vision serves as feedback. Robot-assisted microinjection is an emerging area of research that is capable of improving efficiency, particularly in precision and high-throughput aspects.

Current research into automated cell microinjection has been significant, but challenges remain such as cell fixation during injection. Liu et al. made six symmetrical cylinders to fix the cell, and cell force is calculated according to the displacement of the column during the injection process [7]. Lu et al. adopted a gel cell holder with parallel V-grooves and a machine vision algorithm to identify the number of embryos in a batch and then locate the centerline of each embryo [8]. Xie et al. fabricated continuous and transparent V-shape cell structures on piezoelectric sensors, which can be used for cell injection as well as the detection of injection force in the force control system [9]. Liu et al. used microfluid technology to make some cell holding cavities to patch the cells by the differential pressure between the layer above and below. It is a fabulous solution, but the whole system appears to be quite complicated [10]. In Huang et al., suspended cells were fixed by a specially-designed cell holding device that enabled automatic injection of a batch of suspended cells. To facilitate the pick-and-place process of embryos, holes were embedded in circular profile grooves centered around the geometric center of the holder [11]. In sum, the overall fixing methods are based on negative pressure or the fixation structure. However, most of the methods have a common disadvantage—they all need to

move the cell to a fixed position. However, it is quite difficult to transfer a single cell into a tiny cell device by manual operation.

To solve the problem, this paper introduced a device based on the adhesive effect of the cell and material surface to make cells fixed without a single cell transfer. Polydimethylsiloxane PDMS has been widely used in the biomedical field as a transparent and nontoxic material [12,13]. Recent research has shown that the contact force between PDMS and an object can be modified by improving the chemical property and surface pattern [14–16]. Wang et al. illustrated the relativity of the friction between the PDMS surface array and a PDMS sphere [17]. This result inspiringly offers us new thought into solving the fixation problem of automatic microinjection. Thus, we fixed a single zebrafish embryo cell using an array. We fashioned microcylinders (1700 × 1700) on a PDMS surface (3.5 cm × 3.5 cm). Cylinders were 10 μm apart. By modifying surface topography, the adhesion force between cells and materials was controlled, and during microinjection, liquid drops containing embryonic cells are placed on the PDMS material using a microsuction tube. In comparison with the traditional fixing methods, a single cell transfer operation is not required, and thus the procedure is simplified to a large extent, which benefits the operator significantly.

2. Experimental Methods

2.1. Surface Texturing

To make the PDMS surface array cylinder, craters (1700 × 1700) are created as a mold on the surface of a silicon wafer. After spin-coating photoresistance onto the wafer and setting the pattern, a wafer mold is etched using an Inductively Coupled Plasma (ICP) deep etching system (AMS200, Alcatel, Annecy, France). The corrosion gas is SF_6 (LinDe Gas, Xiamen, China), the protective gas is C_4H_8 (LinDe Gas). Two kinds of gases act on the silicon wafer, and the etching and passivation are carried out. The etching depth is 5 μm.

PDMS was prepared using a Sylgard 184 (Dow Corning Corp., Midland, MI, USA), and a curing agent was made in a ratio of 12:1 *w/w*. The mixture was placed in a desiccator and degassed for 20 min and then poured into a Petri dish and degassed in a vacuum heating furnace at 70 °C for 12 h. A scalpel was used to evenly cut around the pattern, and the PDMS was removed from the silicon mold. Figure 1 depicts the optical microscope image of PDMS.
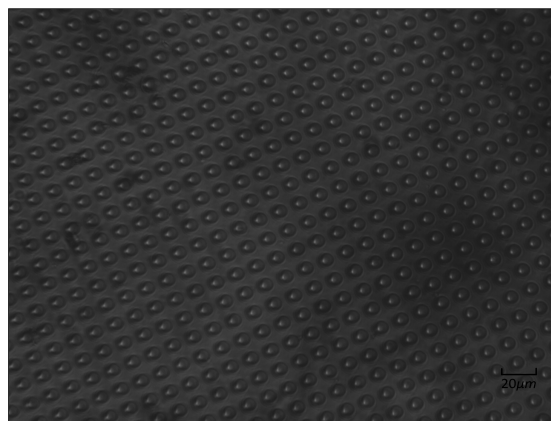

Figure 1. Top-view microscope image of polydimethylsiloxane (PDMS).

2.2. Experimental Setup

We tested the fixed performance of the PDMS. Zebrafish embryo cells have different features that are elastic and require different puncture forces for each developmental stage. So, the 32-cell-stage was selected for the microinjection. PDMS was placed in a culture dish submerged in deionized water 5 mm below the water surface. This was to exclude the interference of fluid and surface tension.

A zebrafish embryonic cell mixture was pulled into a microsuction tube and then dripped on the PDMS. After the cell fell on the PDMS surface, the culture dish was then moved to the microscope (AE31, Motic, Xiamen, China) platform to microinject the targeted embryos. To detect the force of the injection, a force sensor (Nano17, ATI, Apex, NC, USA) was applied between it and the motor. A three-degrees-of-freedom (3-DOF) robotic arm with a 0.04 μm positioning resolution (model: MP-285, Sutter Inc., Novato, CA, USA) drives the injection needle to puncture the cell, and cell injection success or failure was recorded. The experimental injection system appears in Figure 2. The whole procedure is shown in Figure 3; the cell was dripped onto the PDMS surface for the microinjection and transferred away by a suction tube.
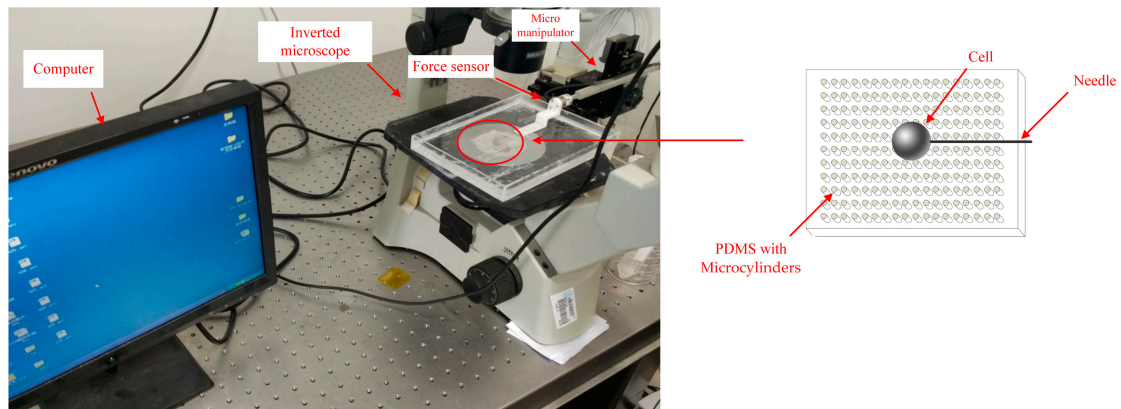

Figure 2. Experimental set-up for zebrafish embryo injection.
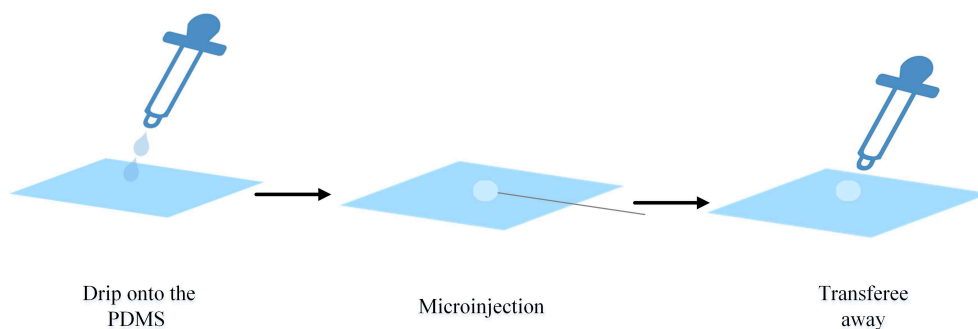

Figure 3. The whole procedure process.

The micropipettes are made from a glass tube with an outer diameter of 1.0 mm and an inner diameter of 0.5 mm (TW100F-4, World Precision Instruments, Sarasota, FL, USA), heated and pulled with the use of a micropipette puller (PC-10, Narishige, New York, NY, USA). The micropipette with a tip diameter of 25 μm after grinding is connected to an automatic pressure microinjector (IM-300, Narishige) via a pressure tube.

In the experiment, the cell was injected from the horizontal direction and tested the fixation effect. The angle was chosen because the cell was most prone to move in this condition. Taking the acceleration process into consideration, the injection needle was set 1 mm away from the cell, and the total travel distance during the injection was 1.7 mm.

3. Results

Different injection velocities were tested 20 times. Video S1 shows the robot-assisted microinjection experiment with the zebrafish embryo at 1.5 mm/s. From Figure 4, we can find that the success rate of puncture obviously rises as the injection speed increases. This was the result of the increasing

acceleration between the embryo and the needle, as well as the interaction force. Injection success was low when the velocity was less than 1 mm/s, and reached 80% at 1.5 mm/s, which meets the application standard of microinjection. A velocity faster than 1.5 mm/s is feasible, so this method has broad application for automated microinjection processes.
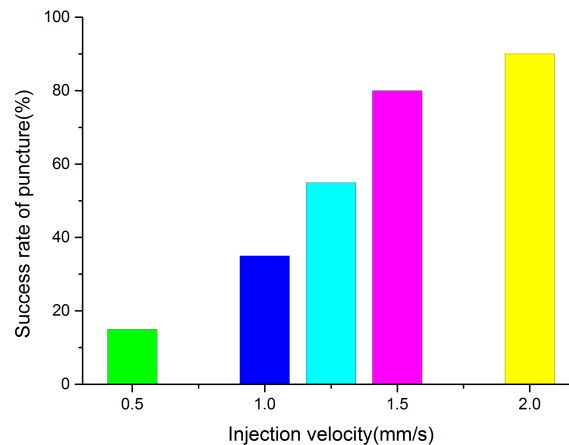
Figure 4. Puncture success rate at different velocities.

A puncture force analysis has been conducted when the velocity is 1.5 mm/s, both in successful and failed cases. Figure 5 shows the case of the contact force between the injection needle and the embryo with a 1.5 mm/s velocity in a failed puncture. The contact force fluctuated when the embryo was exposed to the injection needle and its first movement. This was mainly caused by vibrations of contact and rigid motions. As the injection needle entered the embryo, the embryo membrane was pulled into the embryo, and the contact force between the embryo and the injection needle gradually increased at the same time. When the contact force between the embryo and needle exceeded the contact force between the embryo and the PDMS, the embryo and needle moved together. In this case, the contact force between the embryo and the injection needle was unchanged and both moved together at the same speed.
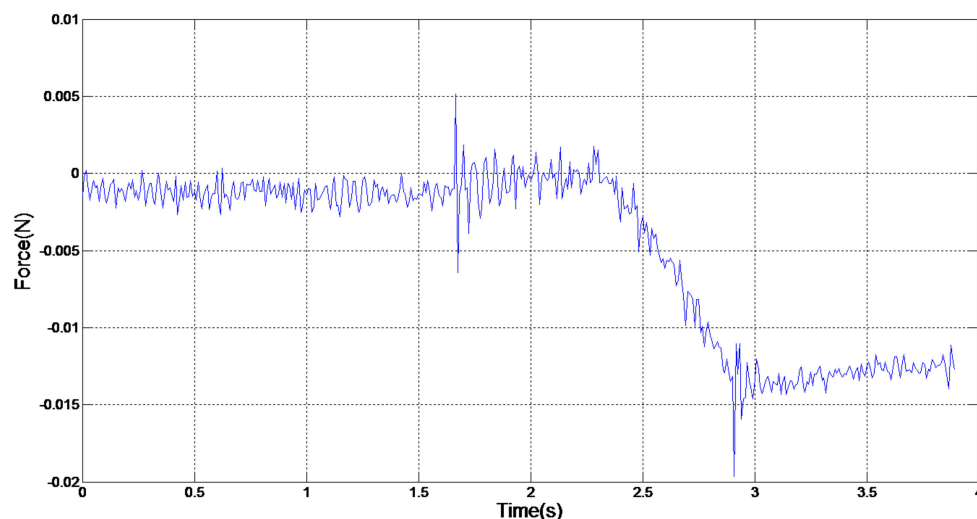
Figure 5. Contact force of failed injection.

Figure 6 shows the classical case of the contact force between the injection needle and the embryo with a 1.5 mm/s velocity in a successful puncture. The contact force gradually increased as the injection needle moved before punctuation and then diminished to indicate successful puncture.
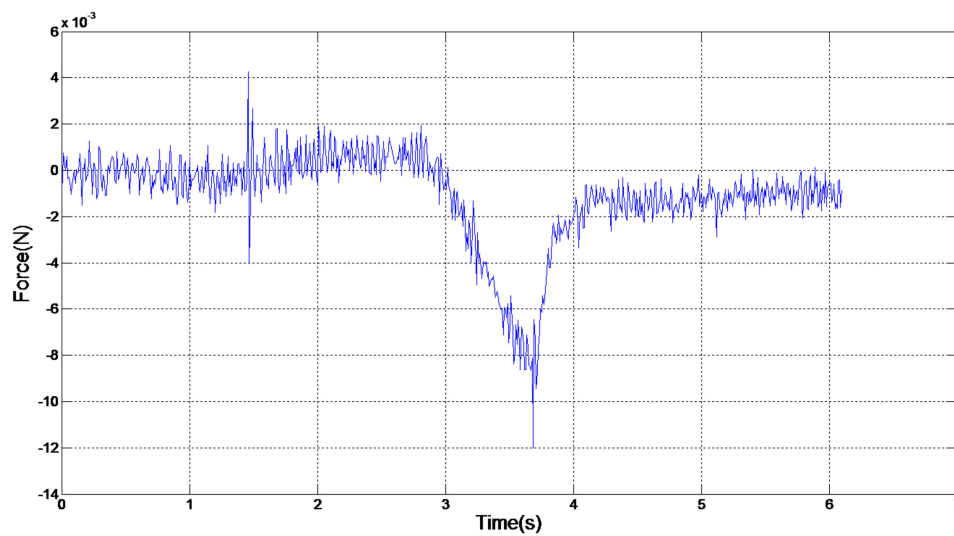
Figure 6. Contact force of successful injection.

From Figures 5 and 6, the key to a successful puncture lies in the embryo puncture force at a certain velocity. In Figure 4, the injection failed, whereas the injection force reached as large as 0.014 N at 1.5 mm/s. However, the embryo was successfully punctured even when the force was 0.009 N at the same velocity. It is normal for a specific zebrafish embryonic embryo to require a large puncture force to penetrate. It is obvious that the adhesion force between the modified PDMS and embryo is limited, and microinjection fails when the injection force exceeds the maximum value of the adhesion force. From the failed group, we calculate 0.0138 N as the maximum value. The diameter of the injection needle also counts in a successful puncture. Less force is needed in the same embryo when the injection needle is thinner. The diameter in usual biomedical experiments is 20 μm, and a size of 25μm is used in this paper; so, the basic standard can be met in practical use. In terms of puncture force, the device we fabricated was again proven to be feasible in robotic microinjection.

4. Conclusions

We fabricated an array cylinder on the light transmitting PDMS material to regulate the force between the material and fixed embryos during automatic zebrafish embryo microinjection. The success rate was 80% when the injection velocity was 1.5 mm/s. The maximum value between the PDMS surface and the cell is 0.0138 N, which meets the requirements in the practical use of robotic microinjection.

Author Contributions: Yunlei Zhou and Xie Yu conceived and designed the experiments; Wenming Xi and Feng Zeng analyzed the data; Songyue Chen contributed materials.

Conflicts of Interest: The authors declare no conflict of interest.

References

1. Morris, A.C.; Eggleston, P.; Cramton, J.M. Genetic transformation of the mosquito Aedesaegypti by micro-injection of DNA. *Med. Vet. Entomol.* **1989**, *3*, 1–7. [CrossRef] [PubMed]
2. Karimirad, F.; Chauhan, S.; Shirinzadeh, B. Vision-based force measurement using neural networks for biological cell microinjection. *J. Biomech.* **2014**, *47*, 1157–1163. [CrossRef] [PubMed]
3. Sun, Y.; Nelson, B.J. Autonomous injection of biological cells using visual servoing. In *Experimental Robotics VII*; Springer: Berlin/Heidelberg, Germany, 2001; pp. 169–178.

4. Sun, Y.; Nelson, B.J. Biological cell injection using an autonomous microrobotic system. *Int. J. Robot. Res.* **2002**, *21*, 861–868. [CrossRef]

5. Wang, W.H.; Liu, X.Y.; Sun, Y. Autonomous zebrafish embryo injection using a microrobotic system. In Proceedings of the 2007 IEEE International Conference on Automation Science and Engineering, Scottsdale, AZ, USA, 22–25 September 2007; pp. 363–368.

6. Huang, H.; Sun, D.; Mills, J.K.; Li, W.J. A visual impedance force control of a robotic cell injection system. In Proceedings of the 2006 IEEE International Conference on Robotics and Biomimetics, Kunming, China, 17–20 December 2006; pp. 233–238.

7. Liu, X.Y.; Kim, K.; Zhang, Y.; Sun, Y. Nanonewton force sensing and control in microrobotic cell manipulation. *Int. J. Robot. Res.* **2009**. [CrossRef]

8. Lu, Z.; Chen, P.C.Y.; Nam, J. A micromanipulation system with dynamic force-feedback for automatic batch microinjection. *J. Micromech. Microeng.* **2007**, *17*, 314. [CrossRef]

9. Xie, Y.; Zhou, Y.L.; Lin, Y.Z.; Wang, L.Y.; Xi, W.M. Development of a Microforce Sensor and Its Array Platform for Robotic Cell Microinjection Force Measurement. *Sensors* **2016**, *16*, 483. [CrossRef] [PubMed]

10. Liu, X.Y.; Sun, Y. Microfabricated glass devices for rapid single cell immobilization in mouse zygote microinjection. *Biomed. Microdevices* **2009**, *11*, 1169–1174. [CrossRef] [PubMed]

11. Huang, H.B.; Sun, D.; Mills, J.K.; Shuk, H.C. Robotic cell injection system with position and force control: Toward automatic batch biomanipulation. *IEEE Trans. Robot.* **2009**, *25*, 727–737. [CrossRef]

12. Chiou, C.H.; Yeh, T.Y.; Lin, J.L. Deformation Analysis of a Pneumatically-Activated Polydimethylsiloxane (PDMS) Membrane and Potential Micro-Pump Applications. *Micromachines* **2015**, *6*, 216–229. [CrossRef]

13. Zhang, L.; Gong, X.; Bao, Y.; Zhao, Y.; Xi, M.; Jiang, C.; Fong, H. Electrospun nanofibrous membranes surface-decorated with silver nanoparticles as flexible and active/sensitive substrates for surface-enhanced Raman scattering. *Langmuir* **2012**, *28*, 14433–14440. [PubMed]

14. Zhou, J.; Khodakov, D.A.; Ellis, A.V. Surface modification for PDMS-based microfluidic devices. *Electrophoresis* **2012**, *33*, 89–104. [CrossRef] [PubMed]

15. Sarvi, F.; Yue, Z.; Hourigan, K. Surface-functionalization of PDMS for potential micro-bioreactor and embryonic stem cell culture applications. *J. Mater. Chem. B* **2013**, *1*, 987–996. [CrossRef]

16. Huang, W.; Wang, X. Biomimetic design of elastomer surface pattern for friction control under wet conditions. *Bioinspir. Biomim.* **2013**, *8*, 046001. [CrossRef] [PubMed]

17. Wang, X.; Wang, J.; Zhang, B. Design principles for the area density of dimple patterns. *Proc. Inst. Mech. Eng. Part J J. Eng. Tribol.* **2015**, *229*, 538–546. [CrossRef]